

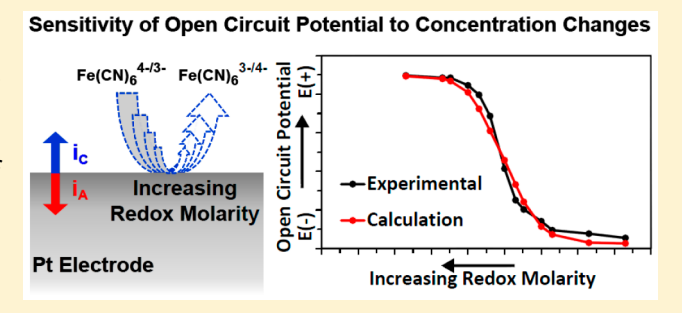
Ultra-Sensitive Potentiometric Measurements of Dilute Redox Molecule Solutions and Determination of Sensitivity Factors at Platinum Ultramicroelectrodes

Stephen J. Percival and Allen J. Bard*

Center for Electrochemistry, Department of Chemistry, The University of Texas at Austin, Austin, Texas 78712, United States

Supporting Information

ABSTRACT: Open circuit potential (OCP) measurements can be very sensitive to small changes in the electrode environment and may allow detection of electron transfer events involving few, and maybe single, electrons. Factors affecting the overall sensitivity of OCP measurements were investigated to achieve the highest sensitivity. The OCP of platinum ultramicroelectrodes (UMEs) was determined in solutions that initially contained only supporting electrolyte where the OCP is a mixed potential governed by background faradaic processes. Then, increasing amounts of a redox couple at equimolar amounts of oxidized and reduced forms were



added. In dilute solutions of the redox couple, the OCP deviates from the redox potential because of additional background half reactions occurring at the electrode. These dominate the OCP through their partial current contributions, shifting the OCP to a mixed potential region. The OCP at a platinum UME remains unchanged from the aqueous electrolyte solution mixed potential until $\sim 10^{-6}$ to 10^{-7} M concentrations of redox molecules are reached. At higher concentrations, the OCP moves toward the formal potential of the redox couple and eventually becomes poised at this value. By using a simple surface modification, the sensitivity to changing concentrations can be increased by almost 2 orders of magnitude. Numerical calculations with a Butler-Volmer formalism can estimate the contribution to the OCP mixed potential from background half reaction currents which are used to extract sensitivity factors from the change in potential with respect to current. The relative sensitivity to changing concentrations is shown to increase as the electrode size decreases.

pen circuit potential (OCP) measurements combined with nanoscale electrodes can be an extremely sensitive detection system and hold the possibility to detect few or even single electron transfer events. We discuss here the sensitivity of the OCP measurement system, factors that can affect the sensitivity, and ways to increase it. This investigation was done by measurement of the changing OCP from a mixed potential system to a poised system as the concentrations of redox molecules increases for various sized electrodes and under different conditions.

The OCP is the potential where zero total current flows in the electrode. The OCP of an electrode immersed in a solution containing sufficient amounts of components of a reversible redox couple will establish an OCP that is the expected thermodynamic potential of the redox couple and is said to be poised at that potential. This is a result of the fast kinetics of both the anodic and cathodic half reactions. Similarly, in solutions containing no reversible redox couple that can establish the electrode potential, other half reactions combine to produce a zero net current, setting the potential of the electrode to the so-called mixed potential of the system. The concept of the mixed potential system has been largely used in corrosion science and was first introduced by Wagner and Traud.^{1,2} Others have shown its use in other areas such as

reaction kinetics³ and catalysis.^{4,5} Additionally, OCP measurements have also been widely applied as sensing techniques for various chemical species.^{6–10} This group recently used this concept as an ultrasensitive nanoparticle detection method and analysis technique where platinum nanoparticles were detected as they collided with a gold electrode, leading to a stepwise change in the measured OCP toward that of bulk platinum.¹¹ By invoking the mixed potential system, the magnitude of the observed OCP steps from nanoparticle collision could be reliably predicted.12

A schematic representation of the concept of the OCP half reactions can be seen in Figure 1. Two different situations are depicted in the schematic, Figure 1A shows a situation where the reaction is not spontaneous $(E_{OX}^{o} - E_{Red}^{o} > 0)$ or is spontaneous but has very slow reaction kinetics where there is a negligible half reaction or mixed current, $i_{\rm mix}$. This system will depend very strongly on kinetics of the half reaction and possible mass transport and is akin to a noble metal electrode placed in an aqueous solution where no redox molecules are present (just electrolyte). Figure 1B shows a situation where

Received: May 16, 2017 Accepted: August 21, 2017 Published: August 21, 2017

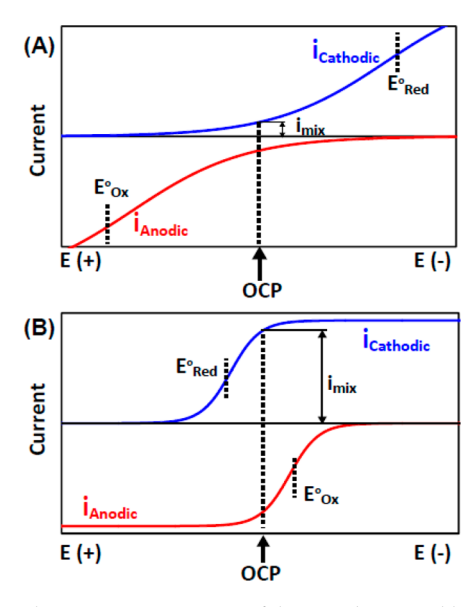
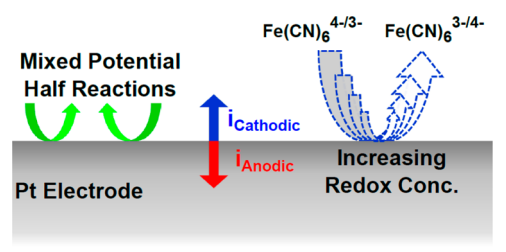


Figure 1. Schematic representation of the mixed potential half reaction i-E curves. (A) When $E_{\text{OX}}{}^{\circ} - E_{\text{Red}}{}^{\circ} > 0$, a system forms that has a very small mixed potential current, i_{mix} (B) When $E_{\text{OX}}{}^{\circ} - E_{\text{Red}}{}^{\circ} < 0$, the reactions will occur spontaneously at the systems OCP and have a more substantial mixed current.

the reaction proceed spontaneously $(E_{\rm OX}{}^{\circ}-E_{\rm Red}{}^{\circ}<0$, e.g., a corrosion reaction where the anodic branch involves iron corrosion and the cathodic one involves oxygen reduction) which has a substantial mixed current, which in principle cannot be directly measured. The electrode potentials for both cases will be decided by the relative rates of the background half reactions. If the system contains a reversible redox couple, the OCP is equivalent to the formal potential of the redox couple and is said to be poised.

The Nernst equation can be used to predict the measured potential of a solution based on the concentrations of ions or redox molecules. The potential of an electrode placed in a solution that contains a mixture of the redox couple can be predicted by the Nernst equation and depends on the relative concentrations of each. At equal concentrations, the measured potential, E, will be poised at the formal potential of the redox couple, $E^{o'}$. However, at very low concentrations of the redox species the Nernst equation no longer applies. The deviation from ideal behavior can be used to determine relative rates of reactions that shift the OCP to the mixed potential region.

Our study shows that at a platinum UME in very dilute redox solutions (equimolar concentrations of K₃Fe(CN)₆ and K₄Fe(CN)₆ were used), the measured OCP is dominated by the background half reactions shifting the observed OCP to a different mixed potential region. Through a series of experiments we determined at what redox concentrations the electrode begins to transition from the mixed potential to the poised potential and we show the shape of the transition can be used to investigate aspects of the OCP that cannot be directly determined, such as the mixed currents. Figure 2 shows a schematic representation of the dilute redox experiment that was performed. The relatively simple experiment involved increasing the concentration of redox couple in various electrolyte solutions and then measuring the resulting OCP at each concentration. The relative rates of electron transfer resulting from each half reaction are represented as arrows in the schematic (where anodic and cathodic currents sum to



E = OCP when $i_{tot} = i_a + i_c = 0$

Figure 2. Schematic showing the generalized dilute redox solution OCP experiment which is a function of mixed potential half reactions and the redox molecule half reactions. The OCP is measured as increasing concentrations of redox molecules are added to the solution. At low concentrations, the OCP is dominated by the mixed potential of the other half reactions but at higher redox concentrations the OCP becomes dominated by the redox molecule and is poised at the formal potential of the redox couple.

zero). Instead of becoming poised at low concentrations the electrode remains at the OCP mixed potential of the solution with just electrolyte present. Furthermore, the electrode does not become poised until a sufficiently high concentration of redox molecules are introduced into the system due to the dominating additional half reactions. As the redox concentration increases, the contribution of the redox half reactions increases and eventually dominates over the background half reactions. As far as we are aware, the only previous study that has observed a concentration dependent deviation from Nernstian behavior for molecules involves an inner-sphere electron transfer reaction, such as O_2 and H_2 . 13

■ EXPERIMENTAL SECTION

Electrode Fabrication. The electrodes used in this study were constructed by sealing either a 25 μ m Pt wire (Alfa Aesar, 99.95% purity) into a borosilicate glass capillary (0.75 mm inner diameter and 1.5 mm outer diameter, Sutter Instrument) under vacuum. After sealing, the electrode was electrically contacted with silver conductive epoxy (Epo-tek H20E, Epoxy Technology, Ted Pella) and NiCr wire. The procedure to prepare the platinum disk nanoelectrodes is described in detail elsewhere. To briefly summarize, a 25 μ m diameter platinum wire was placed in a fused silica capillary tube (o.d., 1 mm; i.d., 0.3 mm, Sutter Instrument Co.) and one end sealed closed using an oxygen/hydrogen flame. The fused silica capillary was then placed in a P-2000 laser pipet puller (Sutter Instrument Co.) and vacuum applied to the unsealed end of the capillary. The laser was used to heat and seal the fused silica around the platinum without pulling the capillary. Then the platinum/fused silica assembly was pulled (pull parameters: heat = 750, filament = 2, velocity = 60, delay = 140, pull = 250) resulting in two ultrasharp tips with the platinum nanowires sealed inside. The Pt wire in the tips was then electrically contacted and carefully polished to expose the disk electrode. The platinum electrode modification was done by soaking the electrode in a 10 mM solution of 1-propanethiol in ethanol for 24 h followed by rinsing it in ethanol then DI water. All solutions were purged with argon before use except when specified otherwise.

Electrochemical Measurements. OCP electrochemical measurements were recorded using a Keithly 6430 high input impedance (>200 $T\Omega$) electrometer operating with a two electrode setup in a faraday cage grounded to the instrument

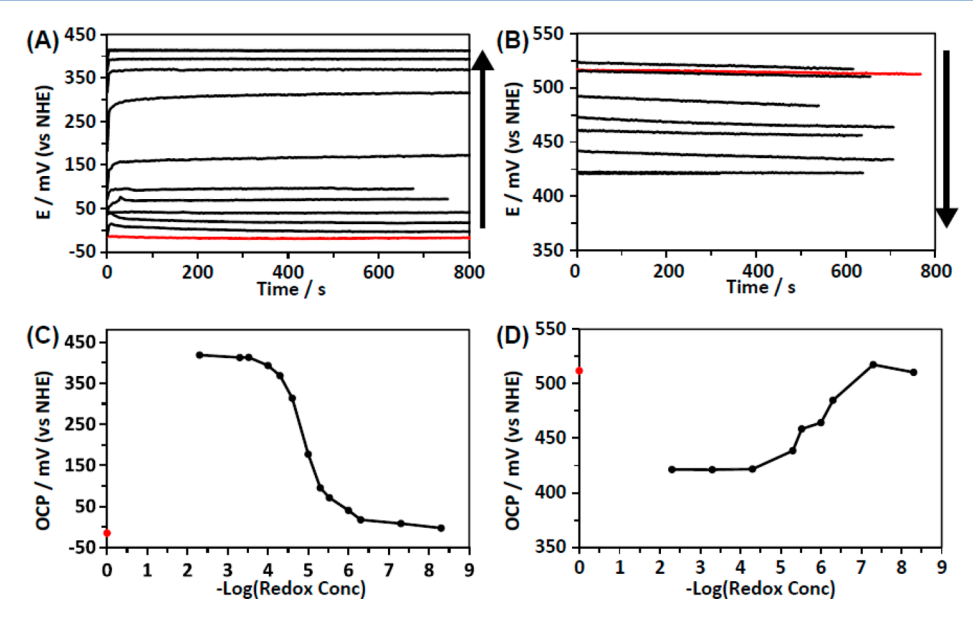


Figure 3. Measured potential over time at a 1.9 μ m radius Pt UME in 100 mM KCl solution that is (A) deaerated by actively purging with argon and (B) air saturated. The arrows in each indicates increasing concentration of added redox molecules from nM to mM and the red curves are the potential curves in the absence of redox molecules, (i.e., pure electrolyte). (C and D) Semi log plots showing the resulting steady state OCP value versus the—log of the redox molecule concentration determined from parts A and B, respectively. The red dots located on the *y*-axis denotes the OCP from the pure electrolyte. A list of redox concentrations used is included in the Supporting Information.

with a shielded triax cable. When performing these types of electrochemical measurements it is important to use a measurement system with a very high input impedance to not affect the resulting measurement. If measurements are made using an instrument with too small of an impedance, erroneous results will be obtained. The data was recorded using an in-house virtual instrumentation program written in LabView (National Instruments) on a desktop PC equipped with a NI GPIB-USB-HS+ (National Instruments) controller and analyzer. A commercial Ag/AgCl reference electrode (CH Instruments) was used for all experiments and all potentials are referenced to NHE.

■ RESULTS AND DISCUSSION

OCP in Dilute Redox Solutions. The OCP experiments were performed by measuring the potential over time (E vs t) of platinum UMEs in various concentrations of redox molecules while the supporting electrolyte remained unchanged. Example OCP measurement experiments can be seen in Figure 3. These were recorded from a 1.9 μ m radius Pt UME in 100 mM KCl in both deaerated (Ar sparged) and air saturated solution. The E vs t plots shown in Figure 3A,B are from the deaerated and air saturated solutions, respectively, and the final portions of the potential curves and are observed to be steady over time. First, the electrode would be allowed to reach a steady state OCP in the electrolyte only solution. This would typically take a long time as there were no redox molecules in solution to poise the potential but would reach a steady OCP faster as the concentration increased. An example of a typical potential curve can be seen in Figure S-2 in the Supporting Information where it took nearly 2 h to reach a steady OCP. After the potential reached a constant potential, the redox couple was injected into the solution and any change in potential was determined.

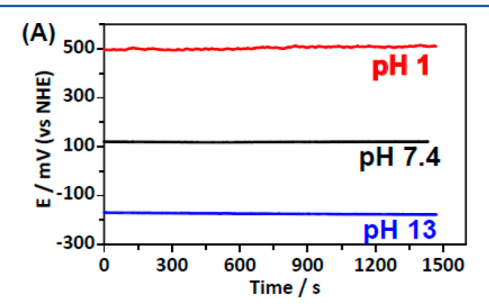
For the deaerated 100 mM KCl solution, Figure 3A, the electrolyte only potential curve is located at a more negative potential. As the redox species, $Fe(CN)_6^{3-/4}$ was added and the

concentration is increased, the potential initially does not change for nM concentrations but as it reaches μ M concentrations, the potential shifts more positive. As the concentration is increased, the change in the measured OCP extends over several orders of magnitude of concentration and does not become poised until the high μ M concentration range (50–500 μ M), after which adding more does not cause further change to the OCP. Figure 3B shows essentially the same trend except for in air saturated solution, where oxygen concentration is much higher, the OCP of the electrolyte starts at a more positive potential than the formal potential of the redox couple and then shifts negatively toward the poised potential as the concentration is increased.

The resulting steady state OCP values that are obtained from each potential curve are plotted versus the negative log of the concentration and shown in Figure 3C,D for the deaerated and air saturated solutions, respectively. These plots show sigmoidal relationships as the OCP goes from being dominated by the mixed potential to becoming poised. The most interesting portion of the curve is the transition region where instead of a sudden transition point there is a more gradual transition. This indicates that in this region the redox half currents and mixed potential half currents, $i_{\rm mix}$ are balanced with each other and one does not quickly dominate over the other. In fact when the relative magnitude of each reaction current are determined from calculations (discussed in detail below), we find that the halfway point in the curve is when the redox and mixed half reaction currents are equivalent.

Having oxygen present in solution caused a large positive shift in the mixed potential because it is removing electrons from the surface of the electrode through the oxygen reduction reaction (ORR). The other half reaction could be water oxidation. To test this, the pH of the solution was changed to both basic and acidic pH. If water oxidation is the other half reaction the mixed potential is predicted to shift by -59~mV/pH, as both the ORR and water oxidation involve protons in their reactions. These tests also confirmed there was not an

effect of the KCl electrolyte as a similar behavior was observed in 100 mM phosphate buffered solution (pH 7.4). Figure 4



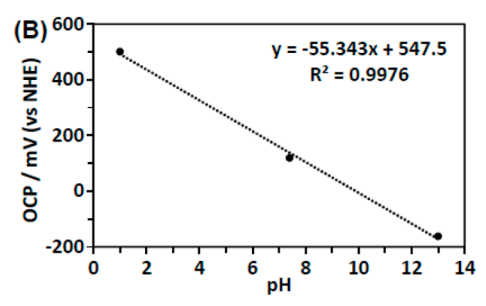


Figure 4. Observed pH dependence on the measured OCP in the electrolyte only solutions. (A) The OCP measured from a 12.5 μ m radius Pt electrode in various pH solutions once it has reached equilibrium. (B) Plot of the measured OCP at equilibrium from (A) as a function of pH. Solutions were 100 mM HCl (pH 1, measured as pH 1.05), 100 mM phosphate buffer (pH 7.4, measured as pH 7.39), and 100 mM KOH + 100 mM KCl (pH 13, measured as pH 12.96), all solutions were Ar sparged for the duration of the experiment.

shows the resulting measured OCP in different pH solutions. As predicted the high pH solution shifted the OCP to more negative potentials whereas the low pH shifted it to more positive potentials. Figure 4B plots the OCP versus pH and from the slope of the line we get a relationship of the OCP to the pH of -55 mV/pH, close to the expected -59 mV/pH.

Numerical Calculations. The contributions from the mixed potential half reactions and the redox half reactions can be calculated from the Butler–Volmer equations for the half reactions. These calculated values were found to closely match the experimental data and can be used to estimate $i_{\rm mix}$ indirectly for each set of conditions. These calculations utilized the Butler–Volmer kinetic equations for the anodic and cathodic currents, which have been shown to effectively model the open circuit mixed potential changes in a previous publication. For generalized half reactions where species O in solution gets reduced to species R, indexed by i to represent a number of different reactions.

$$O_i + n_i e^- \rightleftarrows R_i \quad i = 1, N \quad E_i^0$$
 (1)

We can represent the half reaction currents, i_{Ci} and i_{Aij} for different species of O_i and R_{ij} using eqs 3 and 4 below. ^{12,19}

$$|i_{Ci}| = n_i F A k_{Ci}^{\circ} C_{Oi}(x = 0) \exp[-\alpha_{Ci} f(E - E_{Ci}^{\circ})]$$

 $(i = 1, O_2; i = 3, Fe(CN)_6^{3-})$ (2)

$$|i_{Ai}| = n_i F A k_{Ai}^{\circ} C_{Ri}(x=0) \exp[(1-\alpha_{Ai})f(E-E_{Ai}^{\circ})]$$

$$(i=2, H_2O, i=4, Fe(CN)_6^{4-})$$
(3)

where A is the area of the electrode, n_i is the number of electrons for the overall reaction i, $k_{\text{C}i}^{\text{O}}$ and $k_{\text{A}i}^{\text{O}}$ are the cathodic and anodic rate constants, respectively, for species i. $C_{\text{O}i}(x=0)$ and $C_{\text{R}i}(x=0)$ are the concentrations of the oxidized and reduced forms of the redox couple, $E_{\text{C}i}^{\text{O}}$ and $E_{\text{A}i}^{\text{O}}$ are the standard potentials of the half reactions, α is a symmetry factor, and f=F/RT with R being the gas constant, T is the temperature, and F is Faraday's constant. The concentrations of the redox molecules at the electrode surface can be expressed as eqs 4 and 5.

$$C_{\text{O}i}(x=0) = C_{\text{O}i}^* [1 - i_{\text{C}i}/i_{\text{DC}i}]$$
 (4)

$$C_{Ri}(x=0) = C_{Ri}^* [1 - i_{Ai}/i_{DAi}]$$
 (5)

where $C_{\rm O}^*$ and $C_{\rm R}^*$ are the bulk concentrations of the oxidized and reduced forms of the redox molecule couple and $i_{\rm DC}$ and $i_{\rm DA}$ are the cathodic and anodic diffusion limited currents, respectfully. In the case of a disk shaped UME, the diffusion limited steady state currents can be written in terms of the mass transfer coefficients, $m_{\rm O}$ and $m_{\rm R}$.

$$|i_{\mathrm{DC}i}| = n_i F A m_{\mathrm{O}i} C_{\mathrm{O}i}^* \tag{6}$$

$$|i_{\mathrm{DA}i}| = n_i F A m_{\mathrm{R}i} C_{\mathrm{R}i}^* \tag{7}$$

For a disk electrode, the mass transfer coefficient will be equal to $m_{\rm O}=4D_{\rm O}/\pi r$ and $m_{\rm R}=4D_{\rm R}/\pi r$, with r being the electrode radius and $D_{\rm O}$ and $D_{\rm R}$ the diffusion coefficients of the species O and R, respectively. The equations can be combined into more general expressions.

$$|i_{Ci}| = (k_{Ci}^{\circ}/m_{Oi})(i_{DCi} - i_{Ci}) \exp[-\alpha_{Ci}f(E - E_{Ci}^{\circ}]]$$
 (8)

$$|i_{Ai}| = (k_{Ai}^{o}/m_{Ri})(i_{DAi} - i_{Ai}) \exp[(1 - \alpha_{Ai})f(E - E_{Ai}^{o})]$$
 (9)

The resulting eqs 8 and 9 can be further rearranged to give a more suitable expression for the individual half reaction currents.

$$|i_{Ci}| = i_{DCi} / \left\{ 1 + \frac{m_{Oi}}{k_{Ci}^{\circ}} \exp[-\alpha_{Ci} f(E - E_{Ci}^{\circ})] \right\}$$
 (10)

$$|i_{Ai}| = i_{DAi} / \left\{ 1 + \frac{m_{Ri}}{k_{Ai}^{\circ}} \exp[(1 - \alpha_{Ai})f(E - E_{Ai}^{\circ})] \right\}$$
 (11)

Equations 10 and 11 were used to calculate the currents for each cathodic and anodic half reaction that occurred at the electrode. The potential where all of the calculated anodic and cathodic half currents combine to yield zero net current is the OCP of the electrode, i.e., when the sum of all the cathodic currents equal the sum of all the anodic currents (eq 12).

$$\sum_{i=1}^{N} |i_{C_i}| = \sum_{i=1}^{N} |i_{A_i}| \tag{12}$$

Using eqs 10 and 11 combined with the relationship in eq 12, we calculated OCP values that closely matched the experimental OCP data points in various conditions. When calculating the OCP values under various conditions we used fixed constants for many parameters, most of which are available in the literature. We also decided to use the thermodynamic potentials for the oxygen reduction reaction $(O_2 + 2e^- + 2H^+ \leftrightarrow H_2O_2)$ and the water oxidation reaction $(H_2O \leftrightarrow O_2 + 4H^+ 4e^-)$ for the background half reactions. We should highlight the fact that calculations of the actual rates of

complex inner sphere reactions depend on knowledge of the precise reaction mechanism, which could change the values of E° . The calculations made here can only be considered as effective reaction mechanisms so the true rates may be different than what is calculated.

Figure 5 shows the comparison of experimental OCP curves to the calculated curves for a 12.5 μ m radius electrode. The

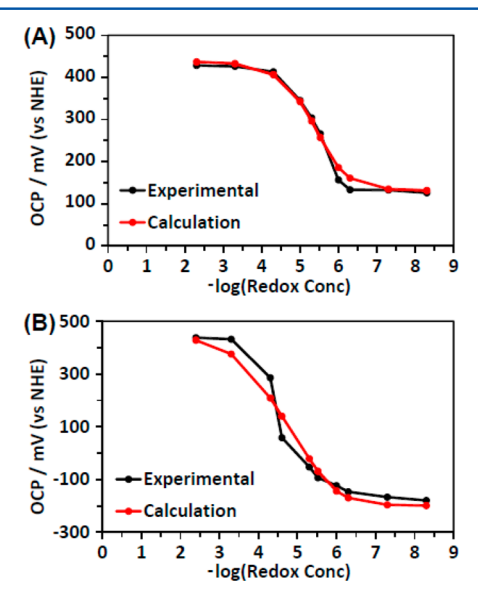


Figure 5. Plots of the OCP curves with different concentrations redox couple from a 12.5 μ m radius Pt electrode in (A) 100 mM phosphate buffer pH = 7.4 and (B) 100 mM KOH + 100 mM KCl. Included for each plot is the resulting calculated data curve using the parameters listed in Table 1 with pH 7.4 for the 100 mM phosphate buffer and 13 for the 100 mM KOH. Both solutions actively bubbled with Ar.

curves were calculated using the set of parameters listed in Table 1 without any changes for all the experimental data shown in Figure 5A,B except for the pH value that is used in the E° values. The close match between the experimental data and the calculated data shows that the model accurately predicts the changing OCP. The different response of the OCP to the increasing redox concentration in 100 mM KOH + 100 mM KCl (pH 13) compared to the 100 mM phosphate buffer (pH 7.4) shows that a higher concentration of redox species is needed to poise the potential in the basic solution. The OCP plot in basic solution does not reach the poised potential until \sim 500 μ M redox concentration. This is due to the pH dependent shift of E° for the water oxidation to lower potential

leading to an increased water oxidation rate in basic solution, which needs to be overcome by the redox species.

Electrode Surface Modification. The background half reactions responsible for shifting the OCP to the mixed potential region are inner-sphere reactions. These reactions can be slowed by a surface bound layer of molecules which will occupy the surface reaction sites, preventing the inner-sphere reaction from occurring and decreasing the magnitude of i_{mix} . It is known that alkanethiols will form self-assembled layers on platinum metal, albeit not as uniformly as on gold.²² Figure 6A is a schematic showing an electrode with a surface bound layer of 1-propanethiol which blocks the inner-sphere reactions from occurring on the electrode surface while still allowing the electron transfer from the outer-sphere redox molecules. This suppression of the magnitude of \hat{i}_{mix} should have the effect of making the system more sensitive to the changing redox concentrations. This inner-sphere blocking effect has been observed previously where short chain alkanethiols will block hydrazine oxidation (inner-sphere) while still allowing ferrocene methanol oxidation to occur (outer-sphere). 23,24

Figure 6B shows the recorded OCP traces from a 12.5 μ m radius Pt electrode that has been modified with 1-propanethiol in deaerated 100 mM PB (pH 7.4). The OCP of the modified electrode in the electrolyte only solution is ~250 mV more positive than compared to the OCP of a bare Pt electrode in electrolyte only (see the Supporting Information Figure S-5B). The more positive OCP is the result of a decreased water oxidation rate on the modified electrode. Both reactions are probably being suppressed but the water oxidation appears to be suppressed more substantially than the oxygen reduction. As the redox concentration is increased, the first OCP change is observed at a much lower concentration. Figure 6C shows the resulting OCP at the different concentrations for the modified electrode and at 5 nM redox concentration, the OCP is similar to the electrolyte solution but at 50 nM redox there is an observed shift in the OCP and is essentially poised at 1 μ M concentration. A comparison of the normalized OCP response for the modified and bare Pt electrodes is shown in Figure 6D. The modified electrode shows greatly increased sensitivity to the changing concentration compared to the bare electrode. The observed change in OCP happens at almost 2 orders of magnitude lower concentrations on the modified electrode. This result demonstrates that the additional background half reactions can be suppressed, and if they can be pushed low enough the possibility of detecting extremely low concentrations using OCP measurements may become feasible.

Electrode Sensitivities. We have shown that the experimentally measured OCP can be modeled as a mixture

Table 1. Values Used for the Various Constants in the Butler-Volmer Calculations of the Half-Reaction Currents to Determine the OCP at Different Concentrations of Redox Couple^a

	$D \left(\text{cm}^2/\text{s} \right)$	E° (V)	k° (cm/s)	α	$C_{\rm o}~({\rm mol/L})$
$i_{\rm C1}~({\rm O_2~Red})$	1.4×10^{-5b}	$0.70 - 2.3 \left(\frac{RT}{F}\right) \times \text{pH}$	0.0015	0.3	1.5×10^{-6}
i_{A2} (H ₂ O Ox)	2.3×10^{-5c}	$1.23 - 2.3 \left(\frac{RT}{F}\right) \times \text{pH}$	8×10^{-8}	0.75	55.5
$i_{C3} (K_3 Fe(CN)_6)$	7.6×10^{-6d}	0.43	0.01	0.5	variable
$i_{A4} (K_4 Fe(CN)_6)$	6.3×10^{-6d}	0.43	0.01	0.5	variable

^aAppropriate values for electrode radius were used for different electrodes. The parameters in bold were varied between different data sets (i.e., different electrodes) to fit the experimental data as closely as possible. ^bOxygen diffusion coefficient taken from ref 20. ^cWater self-diffusion coefficient taken from ref 21. ^dFerricyanide/ferrocyanide diffusion coefficients taken from ref 19.

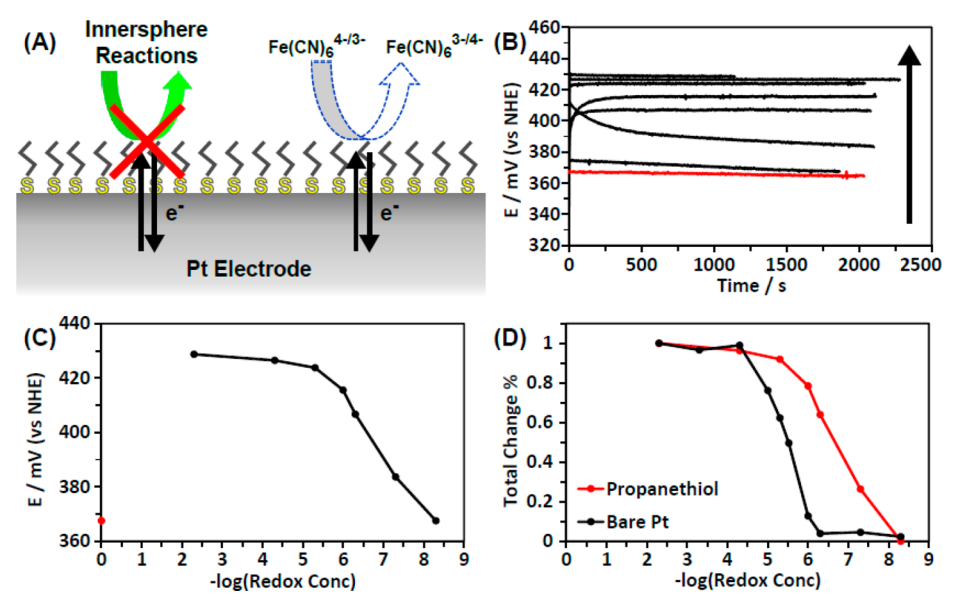


Figure 6. (A) Blocking effect of a surface bound monolayer of 1-propanethiol on inner-sphere reactions. (B) Plot of the resulting OCP vs time curves from a 1-propanethiol surface modified 12.5 μ m radius Pt electrode in deaerated 100 mM PB (pH 7.4) with increasing concentrations of redox couple, indicated by the arrow. (C) Semi log plot of the resulting steady state OCP values for the curves seen in part B. (D) Normalized plots showing the percent change with concentration for the propanethiol modified electrode and a bare Pt electrode. The red curve in part B and the red dot in part C correspond to the electrolyte only.

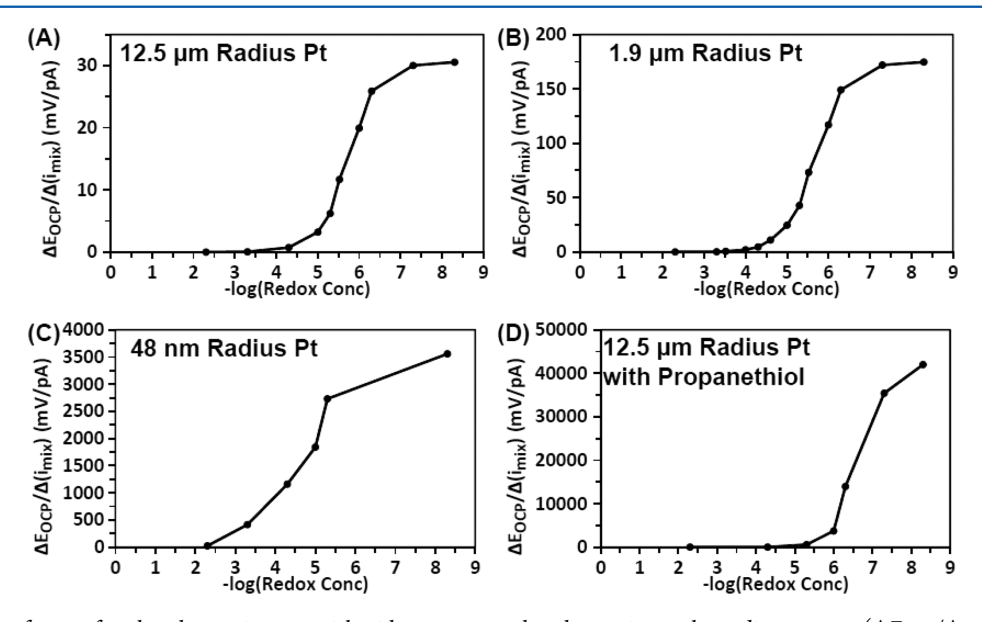


Figure 7. Sensitivity factors for the change in potential with respect to the change in total anodic currents ($\Delta E_{\rm OCP}/\Delta i_{\rm mix}$) versus the redox concentration for (A) the bare 12.5 μ m radius Pt electrode from Figure 5A, (B) 1.9 μ m radius Pt electrode, (C) a 48 nm radius Pt electrode, and (D) a propanethiol modified 12.5 μ m radius Pt electrode. Partial currents were obtained from the calculated half reactions.

of reactions occurring at the electrode surface. The calculation also allows the determination of the relative half currents that each reaction is producing at the OCP for a given set of conditions. By extracting these half currents from the numerical calculations, a sensitivity plot can be made from the change in the mixed current, $i_{\rm mix}$, which is the total of either the anodic or cathodic currents (from the relationship in eq 12, the sum of the anodic currents equals the sum of the cathodic currents).

The OCP change with respect to the changing mixed currents in response to the added redox couple can be thought of as a sensitivity factor $(\Delta E_{\rm OCP}/\Delta i_{\rm mix})$. This factor is a quantifiable measure of how sensitive an electrode will be to very minute changes in the system. Figure 7 shows plots of the

sensitivity factors derived from the calculation for different electrodes. Figure 7A is for the bare 12.5 μ m radius electrode in deaerated 100 mM phosphate buffer. Figure 7B,C is derived from the 1.9 μ m electrode and a 48 nm radius Pt electrode, respectively (both in deaerated 100 mM KCl and the comparisons of the experimental and calculation data are shown in the Supporting Information). Figure 7D is the sensitivity plot for the 1-propanethiol modified 12.5 μ m radius electrode in deaerated 100 mM phosphate buffer. The plots show similar shapes where at the lowest concentrations the sensitivity is the highest followed by a decrease in the sensitivity that trends toward zero at the higher concentrations where the electrodes become poised. The overall shape of the curve

(being most sensitive at the lowest concentrations) is due to the extremely small current changes associated with the extremely small amounts of redox molecules present in solution. These extremely small currents lead to large sensitivities, even when the associated change in potential is small. The sensitivity is seen to increase as the radius of the electrode decreases. The smaller 1.9 μ m radius Pt electrode is more sensitive than the larger bare 12.5 μ m radius electrode where there is an almost 6 times increase in the sensitivity but the 48 nm radius electrode has a maximum sensitivity of more than 20 times that observed for the 1.9 μ m radius Pt electrode. The propanethiol modified electrode had the highest sensitivity where there is an increase in sensitivity by more than 3 orders of magnitude over the bare electrode and it is 10 times more sensitive than the 48 nm electrode.

CONCLUSION

Measurements of the OCP at platinum UMEs revealed relative sensitivities of the electrodes to changing redox concentrations in solutions of dilute redox molecules. By investigating dilute redox solutions, we found the OCP depends on the multiple half reactions occurring at the electrode surface and that the change in the OCP can be predicted through numerical calculations. There is a concentration range where the OCP goes from being dominated by the mixed potential half reactions of water oxidation and oxygen reduction to being poised at the redox molecule formal potential. By modeling the experimentally observed OCP values using a simple Butler-Volmer formalism we could extract the partial currents and derive sensitivity factors. These modeled OCP values matched very well with the observed values. We have also shown that surface modification of the electrode with a simple adsorbed monolayer can block the inner-sphere background half reactions. This has the effect of decreasing the magnitude of $i_{\rm mix}$ and increasing the sensitivity to the changing concentration by almost 2 orders of magnitude and the sensitivity factor by 3 orders of magnitude.

ASSOCIATED CONTENT

S Supporting Information

. The Supporting Information is available free of charge on the ACS Publications website at DOI: 10.1021/acs.analchem.7b01856.

Chemicals used, mass transfer limited current CVs of the Pt UMEs, example potential vs time curve, experimental and calculated OCP curves for the 1.9 μ m radius Pt electrode and for a 48 nm radius Pt electrode, and nonnormalized OCP curves comparing the modified and bare platinum electrodes (PDF)

AUTHOR INFORMATION

Corresponding Author

*Phone: (512) 471-3761. E-mail: ajbard@mail.utexas.edu.

ORCID ®

Allen J. Bard: 0000-0002-8517-0230

Notes

The authors declare no competing financial interest.

ACKNOWLEDGMENTS

We gratefully acknowledge the financial support from the National Science Foundation (Grant CHE-1405248 to A.J.B.) and the Welch Foundation (Grant No. F-0021).

REFERENCES

- (1) Wagner, C. W.; Traud, W. Z. Elektrochem. 1938, 44, 391-402.
- (2) Wagner, V. C.; Traud, W. Corrosion 2006, 62, 843-855.
- (3) Andersen, T. N.; Eyring, H. J. Phys. Chem. 1963, 67, 92-97.
- (4) Spiro, M. J. Chem. Soc., Faraday Trans. 1 1979, 75, 1507-1512.
- (5) Roberts, J. A. S.; Bullock, R. M. Inorg. Chem. 2013, 52, 3823-3835.
- (6) Gao, L. J.; Conway, B. E. J. Electroanal. Chem. 1995, 395, 261–
- (7) Sekhar, P. K.; Brosha, E. L.; Mukundan, R.; Nelson, M. A.; Williamson, T. L.; Garzon, F. H. Sens. Actuators, B 2010, 148, 469–477
- (8) Lu, G.; Miura, N.; Yamazoe, N. J. Mater. Chem. 1997, 7, 1445-1449.
- (9) Schönauer, D.; Wiesner, K.; Fleischer, M.; Moos, R. Sens. Actuators, B 2009, 140, 585-590.
- (10) Vallières, C.; Gray, J.; Poncin, S.; Matlosz, M. Electroanalysis 1998, 10, 191–197.
- (11) Zhou, H.; Park, J. H.; Fan, F.-R. F.; Bard, A. J. J. Am. Chem. Soc. **2012**, 134, 13212–13215.
- (12) Park, J. H.; Zhou, H.; Percival, S. J.; Zhang, B.; Fan, F.R. F.; Bard, A. J. *Anal. Chem.* **2013**, *85*, 964–970.
- (13) Warner, T. B.; Schuldiner, S. J. Electrochem. Soc. 1965, 112, 853–856.
- (14) Katemann, B. B.; Schuhmann, W. Electroanalysis 2002, 14, 22–28.
- (15) Li, Y.; Bergman, D.; Zhang, B. Anal. Chem. 2009, 81, 5496–5502.
- (16) Shao, Y.; Mirkin, M. V.; Fish, G.; Kokotov, S.; Palanker, D.; Lewis, A. Anal. Chem. 1997, 69, 1627–1634.
- (17) Cluett, M. L. Anal. Chem. 1964, 36, 2199.
- (18) Pourbaix, M. J. N.; Muylder, J. V.; de Zoubov, N. *Platinum Metals Rev.* **1959**, 3, 47–53.
- (19) Bard, A. J.; Faulkner, L. R. Electrochemical Methods: Fundamentals and Applications, 2nd ed.; John Wiley and Sons: New York, 2001; Chapter 3.
- (20) Hsueh, K.-L.; Gonzalez, E. R.; Srinivasan, S. Electrochim. Acta 1983, 28, 691-697.
- (21) Holz, M.; Heil, S. R.; Sacco, A. Phys. Chem. Chem. Phys. 2000, 2, 4740-4742.
- (22) Love, J. C.; Estroff, L. A.; Kriebel, J. K.; Nuzzo, R. G.; Whitesides, G. M. Chem. Rev. 2005, 105, 1103–1169.
- (23) Bard, A. J. J. Am. Chem. Soc. 2010, 132, 7559-7567.
- (24) Xiao, X.; Pan, S.; Jang, J. S.; Fan, F.-R. F.; Bard, A. J. J. Phys. Chem. C 2009, 113, 14978–14982.